Journal of Information Display, vol. 4, no. 1, 2003

Anchoring Properties in Photo-aligned Periodic Domains for Wide-viewing Liquid Crystal Displays

Chang-Jae Yu[**], **Jae-Hong Park**[**], **and Sin-Doo Lee**[*]

Abstract

We studied the anchoring properties in photo-aligned periodic domains of liquid crystals (LCs) in an alternating homeotropic and hybrid geometry. In this geometry, the surface anchoring energy was determined in using the director-distorted length of the LC near domain boundary, calculated in a linear approximation of the director profile within the continuum theory. The measurements were made using the LC diffraction grating with the phase profile in the form of a trapezoid.

Keywords : anchoring energy, continuum theory, diffraction grating, far-field diffraction.

1. Introduction

In liquid crystal (LC) devices including liquid crystal displays, the interaction of the LC molecules with treated glass substrates is a key issue as electro-optic response of the LC devices may be strongly influenced by the surface anchoring. The surface anchoring energy is one of the important factors that characterizes the surface orientation of the LC molecules. A variety of techniques, such as the wedge-cell method [1,2], the external field method [3,4], and the fully leaky waveguide method [5,6], have been used for measuring the anchoring energy. With the exception of the wedge-cell method in the absence of an external field, complicate mathematics to determine the anchoring energy.

In this work, we studied the anchoring properties in photo-aligned periodic domains of LCs in an alternating homeotropic and hybrid geometry as shown in Fig. 1. In this geometry, it was found that the linearly distorted length induced by the boundary effect between the homeotropic and hybrid domains was expressed in terms of the extrapolation length defined as the ratio of the effective elastic constant to the surface anchoring strength. From the measurements of the diffraction patterns of a quasi-binary grating, the anchoring energy was determined using the phase profile in the form of a trapezoid [7]. It is important to understand the anchoring properties of the LC in periodic domains for developing wide-viewing LC displays.

2. LC Director Profile

In the continuum theory [8], the LC director-profiles are linearly varied along the y- and z-axes near the domain boundary between the homeotropic and hybrid domains in the coordinate system as shown in Fig. 1. Assuming that the LC molecules lie on the xz-plane, the tilt angle θ of the LC molecules minimizing the total free energy in the linearly distorted region is expressed as

$$\theta(y,z)=\frac{\pi}{2}-\frac{\pi}{2wd}(w-y)(d-z), \quad (1)$$

where the cell thickness and the linearly distorted length are denoted by d and w, respectively. Fig. 2 shows the tilt angle profile of the LC molecules calculated from Eq. (1).

Manuscript received February 11, 2003; accepted for publication March 21, 2003.
This work was supported in part by Ministry of Information and Communication under the Advanced Backbone IT technology development project.
*Member, KIDS; **Student Member, KIDS.
Corresponding Author : Chang-Jae Yu
School of Electrical Engineering #032, Seoul National University, Gwanak P.O. Box 34, Seoul 151-742, Korea.
E-mail : sidlee@plaza.snu.ac.kr **Tel** : +2 880-1823 **Fax** : +2 874-9769

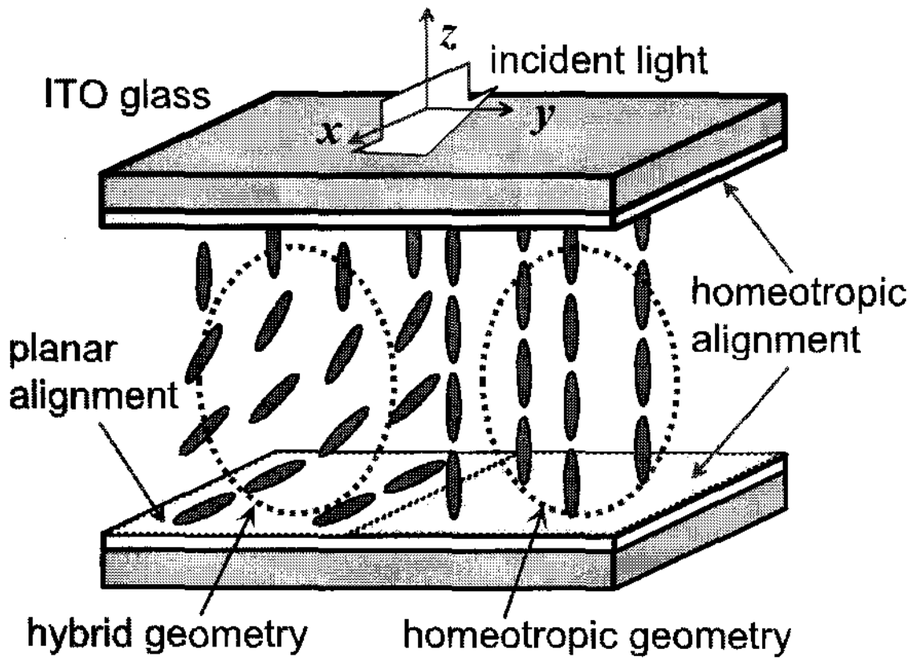

Fig. 1. The LC cell structure having alternating homeotropic and hybrid domains.

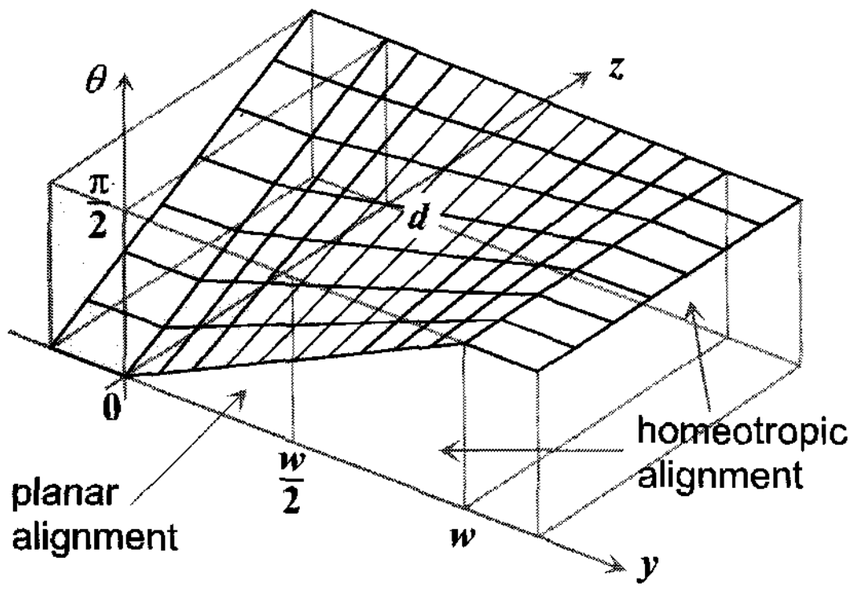

Fig. 2. The tilt angle profiles of the LC molecules near the domain boundary with the linearly distorted length w and the cell thickness d.

As shown in Fig. 2, the planar alignment was found to be present in the region of $y \leq w/2$ and the homeotropic alignment was present in the region of $y \geq w/2$ and at the bottom substrate at $z = 0$. Throughout the entive region of the top substrate at $z = d$, the homeotropic alignment layer was present. This means that the hybrid and homeotropic domains were produced in the regions below and above w/2, respectively. In the range of $0 \leq y \leq w$, the LC director was linearly twisted along the y-axis due to curvature elasticity [8]. Using the Rapini-Papoular model [9] in the one elastic constant approximation, the total free energy in the linearly distorted region in the yz-plane can be expressed as

$$F = \frac{\pi^2 K_{eff}}{24wd}\left(d^2 + w^2\right) + \frac{\pi - 2}{4\pi} w W_p, \qquad (2)$$

where Keff and Wp are the relevant elastic constant and the zenithal (or polar) anchoring strength, respectively. Minimizing Eq. (2) with respect to w, we obtain the linearly distorted length w as follows

$$w = d\left[1 + \frac{6}{\pi^3}(\pi - 2)\frac{d}{\zeta}\right]^{-\frac{1}{2}}, \qquad (3)$$

where ζ is the extrapolation length [8] defined as K_{eff}/W_p. In fact, the extrapolation length ζ is directly related to the linearly distorted length w, determined from the measured diffraction patterns of the LC binary grating with a linearly graded phase profile as described later.

3. Diffraction Patterns

From the tilt angle profiles shown in Fig. 2, the phase profiles along the y-axis can be calculated using the effective refractive index and the Jones matrix formalism [10]. In general, in order to obtain the diffraction patterns of the LC grating with such phase profile, the fast Fourier transformation [11] with the linearly distorted length w is required.

Let us assume that the phase shift passing through the LC layer changes linearly along the y-axis in the distorted region near the domain boundary. In this case, the distorted length w can be easily obtained using the far-field diffraction formula [11] of the LC grating with the help of linearly graded phase profiles as shown in Fig. 3. Here, the length of w is equivalent to that in Fig. 2. From the far-field diffraction formula, the non-diffraction (zero-th order diffraction) efficiency, η_0, is expressed as

$$\eta_0 = \left[(1 - 2\xi)\cos(\Delta\phi) + 2\xi\,\mathrm{sinc}(\Delta\phi)\right]^2 \qquad (4)$$

and the k-th order diffraction efficiency, η_k (k non-zero integers), is

$$\eta_k = \left[\xi\Phi_+ - \frac{1}{\pi k}\Psi_-\right]^2 \cos^2\left(\frac{\pi k}{2}\right) + \left[\xi\Phi_- - \frac{1}{\pi k}\Psi_+\right]^2 \sin^2\left(\frac{\pi k}{2}\right), \qquad (5)$$

where $\xi = w/L$, $\Delta\phi = (\phi_e - \phi_o)/2$, and

$$\begin{aligned} \Phi_{\pm} &= \operatorname{sinc}(\Delta\phi + \pi k\xi) \pm \operatorname{sinc}(\Delta\phi - \pi k\xi), \\ \Psi_{\pm} &= \sin(\Delta\phi + \pi k\xi) \pm \sin(\Delta\phi - \pi k\xi). \end{aligned} \tag{6}$$

For $\xi = 0$ ($w = 0$), Eq. (4) can be simply expressed as

$$\eta_0^* = \frac{1+\cos(\Delta\phi)}{2}. \tag{7}$$

Similarly, the k-th order diffraction efficiency, η_k^* is

$$\eta_k^* = \frac{1-\cos(\Delta\phi)}{2}\operatorname{sinc}^2\left(\frac{\pi k}{2}\right). \tag{8}$$

The above equations (7) and (8) correspond to the diffraction efficiencies of an ideal binary grating [11]. Note that for an ideal binary grating, no diffraction occurs at even-order apart from the relative phase difference $\Delta\phi$ in Eq. (8). From the least-square-fits of the diffraction patterns to Eqs. (4) and (5) using the convolution theorem [11], the parameter $\xi = w/L$ can be determined.

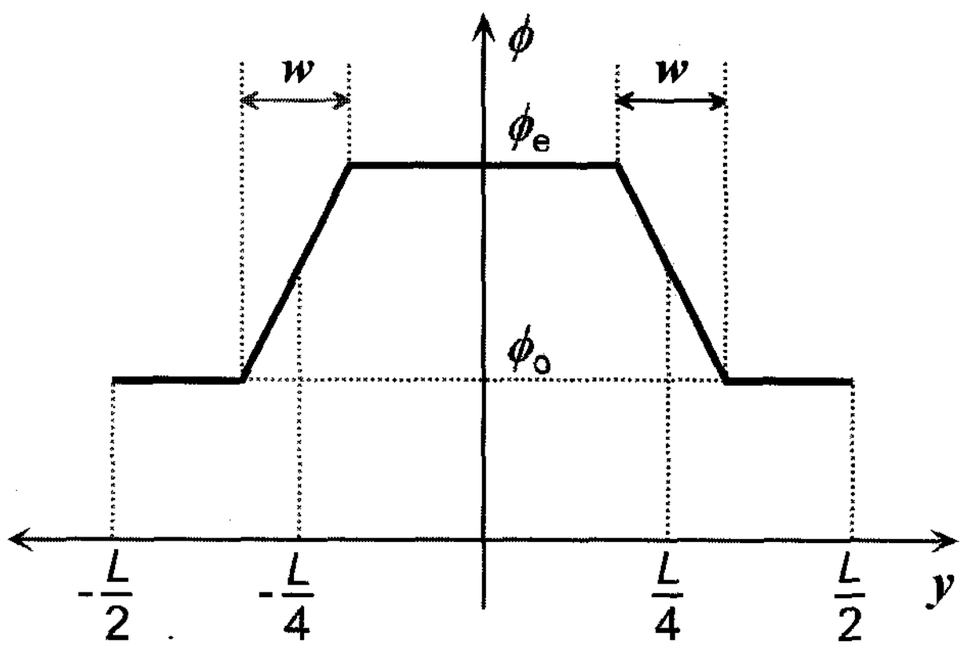

Fig. 3. The phase profiles of the LC grating in the form of a trapezoid with the grating period of L. The phase shifts through the undistorted homeotropic and hybrid regions in the LC layer are denoted by ϕ_o and ϕ_e, respectively. The linearly distorted length near the domain boundary is denoted by w.

4. Experiments

The LC binary gratings were made using glass substrates coated with a photopolymer of LGC-M1 (LG Cable Ltd., Korea) [12]. The photopolymer, aligning the LC molecules homogeneously by the linearly polarized ultraviolet (UV) light exposure and homeotropically by no UV exposure, has cinnamoyl containing photosensitive groups attached to polymethacrylate backbone.

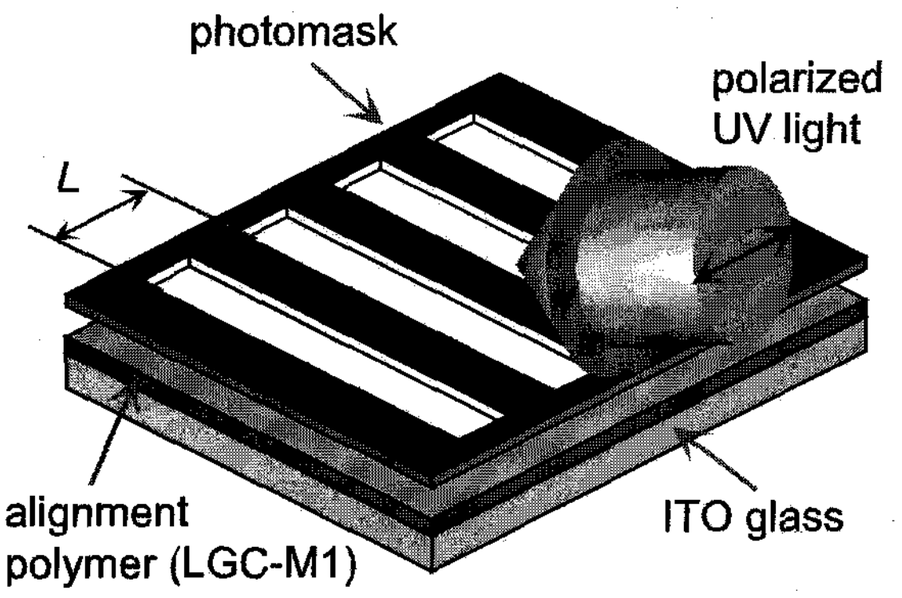

Fig. 4. The preparation of the bottom substrate having alternating homeotropic and planar alignment layers.

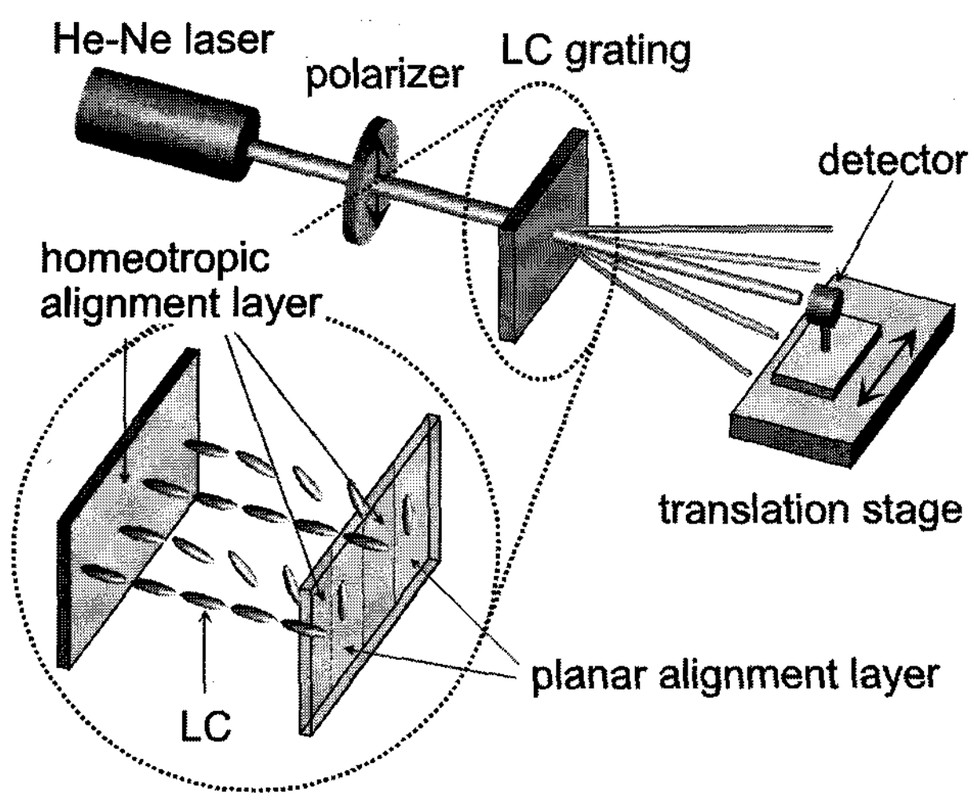

Fig. 5. The experimental setup for measuring the diffraction patterns of the LC grating. The polarization state of the incident light is perpendicular to the direction of the grating vector.

One substrate having alternating striped patterns was prepared though a one-step exposure of the linearly polarized UV light through an amplitude photomask at 2.0 mW for 2 minutes as shown in Fig. 4. The other substrate was not expored to UV. In a single LC cell, various grating periods were obtained using a photomask with different grating periods under the same experimental conditions of the cell thickness and the anchoring energy. The two substrates were assembled

using glass spacer of 6.0 μm thick. The LC material used in this work was the MLC-6012 by Merck.

The polarization state of the incident light is parallel to the x-axis, i.e., perpendicular to the direction of a grating vector (y-axis). In this configuration, the x-polarized light experiences the phase modulation as shown in Fig. 3. A He-Ne laser of 632.8 nm and a motorized translation stage, on which a photo-detector was mounted, were used for measuring the diffraction intensity profiles as shown in Fig. 5. All the measurements were carried out at room temperature.

5. Results and Discussion

Fig. 6 shows the diffraction patterns of the LC binary grating with a grating period L = 19 μm as a function of the normalized distance defined by the unit distance for each order of diffraction. Here, open circles and solid line represent the experimental intensity profiles and the theoretical pattern calculated from Eqs. (4) and (5), respectively. As shown in Fig. 5, the even-order diffractions were somewhat different from those in the ideal binary grating. This is attributed to the periodic boundary effects in terms of the linearly distorted length ξ.

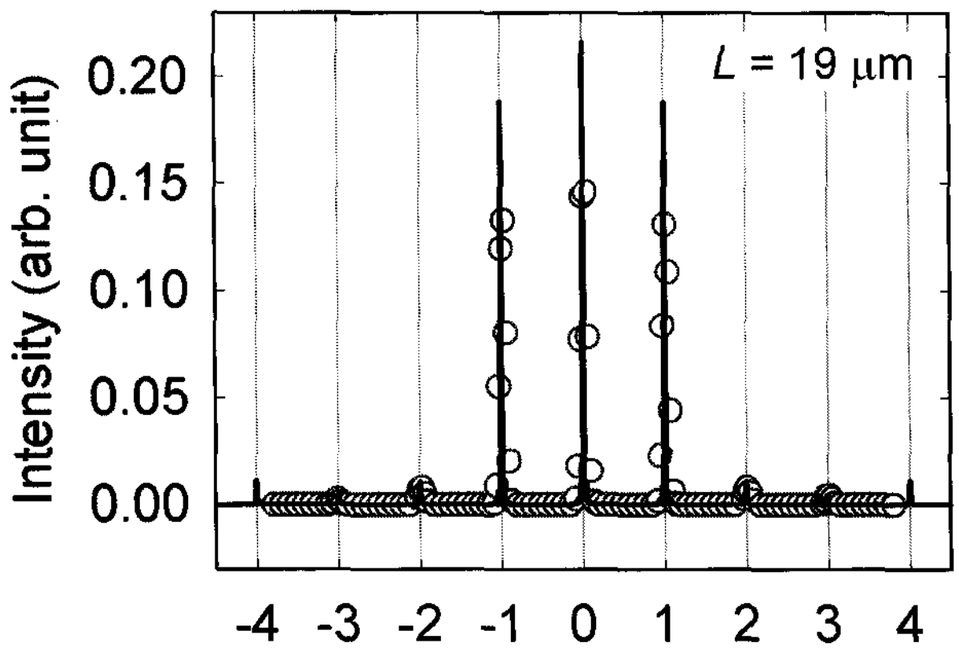

Fig. 6. The measured and calculated diffraction intensity profile of the LC binary grating having a grating period L = 19 μm.

For different grating periods, the parameter ξ, determined from the least-square-fits of experimental data to Eqs. (4) and (5), are shown in Fig. 7 as a function of the inverse grating period (1/L). It was found that the parameter ξ is linearly proportional to the inverse grating period as shown in Fig. 7. The slope of the straight line for ξ was found to corresponds with the actuall distorted length w and to be 2.04 for d = 6.0 μm.

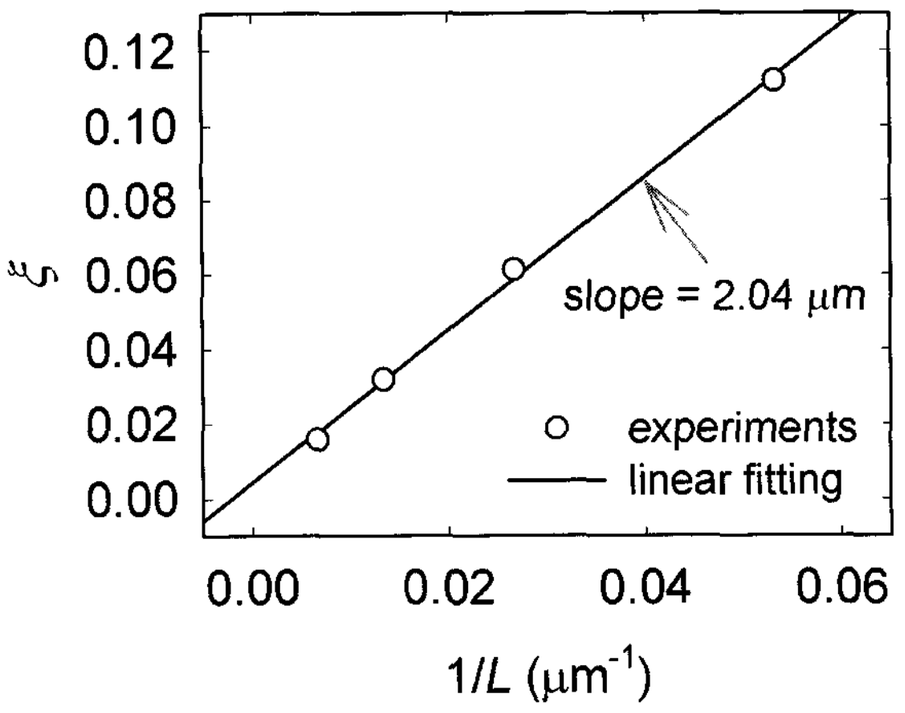

Fig. 7. The distorted parameter ξ, scaled by the grating period L, as a function of (1/L). Open circles were determined from Eqs. (4) and (5) for various grating periods and solid line represents the least-squares-fit of the data to a straight line.

With the parameters, w = 2.04 μm and d = 6.0 μm, the extrapolation length ζ was calculated to be 1.73×10^{-7} in SI unit by using Eq. (3). Applying the typical value of the relevant elastic constant, $K_{eff} = 10^{-11}$ N, the zenithal (or polar) anchoring strength W_p was estimated as 5.78×10^{-5} J/m^2, which can be considered to be physically reasonable.

6. Conclusion

We studied the periodic boundary effect on the anchoring properties of the LC binary grating having alternating homeotropic and hybrid domains. In this configuration, the linearly distorted length, determined from the measured diffraction patterns of the LC binary grating with a linearly graded phase profile, was directly related to the cell thickness and the extrapolation length. The polar anchoring strength was evaluated using the extrapolation length calculated from the linearly distorted length.

In summary, we developed a simple method of fabricating binary LC gratings that are useful for producing periodic multi-domains and determining the anchoring properties of the LC. Moreover, this technology would be applicable for improving the

viewing characteristics of the LC displays with multi-domains.

References

[1] D. Riviere, Y. Levy, and E. Guyon, J. Phys. (France) Lett. **40**, L215 (1979).

[2] G. Barbero, N. V. Madhusudana, and G. Durand, J. Phys. (France) Lett. **45**, L613 (1984).

[3] K. H. Yang, J. Appl. Phys. **53**, 6742 (1982).

[4] H. Yokoyama and H. A. van Sprang, J. Appl. Phys. **57**, 4520 (1985).

[5] F. Yang, J. R. Sambles, Y. Dong, and H. Gao, J. Appl. Phys. **87**, 2726 (2000).

[6] F. Yang, L. Ruan, and J. R. Sambles, J. Appl. Phys. **88**, 6175 (2000).

[7] C.-J. Yu, J.-H. Park, J. Kim, M.-S. Jung, and S.-D. Lee, to be published (2003).

[8] P. G. de Gennes and J. Prost, The Physics of Liquid Crystals, 3rd ed. (Oxford University Press, New York, 1993).

[9] A. Rapini and M. J. Papoular, J. Phys. (Paris) Colloq. **30**, C4-54 (1969).

[10] I.-C. Khoo and S.-T. Wu, Optics and Nonlinear Optics of Liquid Crystals (World Scientific Publishing Co., Singapore, 1993).

[11] J. W. Goodman, Introduction to Fourier Optics, 2nd ed. (McGraw-Hill Book Co., Singapore, 1996).

[12] J. Kim, S. Kim, K. Park, and T. Kim, 2001 SID International Symposium Digest of Technical Papers (Society for Information Display, San Jose, 2001), p. 806.